Quantum Interference in Electron-Hole Generation in Noncentrosymmetric Semiconductors

J. M. Fraser, A. I. Shkrebtii, J. E. Sipe, and H. M. van Driel
Department of Physics, University of Toronto, Toronto, Canada M5S 1A7
(Received 9 April 1999)

We show that, when fundamental optical beams are present in a noncentrosymmetric medium simultaneously with their sum-frequency beam, quantum interference between single- and two-photon transitions modifies the net absorption, if the sum frequency corresponds to an energy greater than the band gap. At a macroscopic level this effect can be related to the imaginary part of a second-order susceptibility and can be used to coherently control carrier populations and optical absorption. We illustrate this novel effect using phased 1550 and 775 nm, 120 fs pulses incident on GaAs at 295 K.

PACS numbers: 78.47.+p, 42.65.–k, 78.55.Cr

The field of nonlinear laser optics dates from the observation of second-harmonic generation in crystalline quartz [1]. Although a myriad of nonlinear optical processes have been discovered since then [2–4], second-order (χ_2) processes such as sum- and difference-frequency mixing continue to capture most of the interest. Of necessity χ_2 is nonzero only in noncentrosymmetric media, such as certain crystals. When such a crystal is transparent at all frequencies involved, χ_2 is real and the crystal can act as an optical "catalyst" to convert incident energy into new optical frequencies. If, however, the crystal is absorbing for at least one of the frequencies, the imaginary component of χ_2 ($\mathrm{Im}[\chi_2]$) is nonzero. In the case of sum-frequency generation, it is generally believed [5] that $\mathrm{Im}[\chi_2]$ plays no role in energy absorption. Here we demonstrate that when coherent fundamental and sum-frequency beams are *simultaneously* present in a crystal, and if the sum frequency falls in a region of band absorption, $\mathrm{Im}[\chi_2]$ can contribute to the *removal* of energy from *all* beams. This is due to the interference of single- and two-photon absorption pathways. This effect can be used in an active sense to coherently control optical transmission and band populations through the relative phase of the fields. We experimentally demonstrate this new effect in bulk GaAs at 295 K, and explicitly discriminate its origin and nature from the coherent control of current injection in semiconductors [6].

To illustrate the underlying physics, we consider phase-related and temporally overlapped pulses of frequency ω and 2ω, with $2\hbar\omega > E_g > \hbar\omega$, interacting with a noncentrosymmetric crystal with direct gap E_g. The extension to the general sum-frequency case is straightforward. In the presence of the electric field $\mathbf{E}(t) = [\mathbf{E}(\omega)\exp(-i\omega t) + \mathbf{E}(2\omega)\exp(-2i\omega t)] + \text{c.c.}$, there are both one- and two-photon amplitudes for the excitation of the crystal from its ground state $|0\rangle$ to a state $|cv\mathbf{k}\rangle$ in which an electron-hole pair (in conduction and valence bands c and v, respectively) is created at crystal momentum $\mathbf{k}$. Writing the state of the crystal as

$$|\Psi(t)\rangle = c_0(t)\,|0\rangle + \sum_{cv\mathbf{k}} c_{cv\mathbf{k}}(t)\,|cv\mathbf{k}\rangle,$$

a straightforward Fermi's Golden Rule calculation using the minimal coupling Hamiltonian $(A \cdot p)$ [6] yields a rate $\dot{n}$ for the generation of electron-hole pairs per unit volume,

$$\dot{n} = \frac{1}{V}\sum_{cv\mathbf{k}} \frac{d}{dt}[|c_{cv\mathbf{k}}(t)|^2] = \frac{2\pi}{V}\sum_{cv\mathbf{k}} |K_{cv\mathbf{k}}|^2 \delta(\omega_{cv}(\mathbf{k}) - 2\omega). \quad (1)$$

Here V is the normalization volume, the energies of the conduction and valence bands are $\hbar\omega_c(\mathbf{k})$ and $\hbar\omega_v(\mathbf{k})$, respectively, $\omega_{cv}(\mathbf{k}) \equiv \omega_c(\mathbf{k}) - \omega_v(\mathbf{k})$, and

$$K_{cv\mathbf{k}} = \frac{ie[\mathbf{p}_{cv}(\mathbf{k})\cdot\mathbf{E}(2\omega)]}{m\hbar\omega_{cv}(\mathbf{k})} + \left(\frac{2ie}{m\hbar\omega_{cv}(\mathbf{k})}\right)^2 \times \sum_n \frac{[\mathbf{p}_{cn}(\mathbf{k})\cdot\mathbf{E}(\omega)][\mathbf{p}_{nv}(\mathbf{k})\cdot\mathbf{E}(\omega)]}{\bar{\omega}_{cv}(\mathbf{k}) - \omega_n(\mathbf{k})},$$

is the sum of one- and two-photon amplitudes, where $\mathbf{p}_{cv}(\mathbf{k})$ is the momentum matrix element between the valence and conduction band states, n ranges over all bands, and $\bar{\omega}_{cv}(\mathbf{k}) \equiv [\omega_c(\mathbf{k}) + \omega_v(\mathbf{k})]/2$. Squaring $K_{cv\mathbf{k}}$ in Eq. (1) leads to three contributions to $\dot{n}$ viz. $\dot{n} = \dot{n}_{2\omega} + \dot{n}_\omega + \dot{n}_I$; the first two contributions are purely one- and two-photon terms, respectively, involving only the associated amplitudes, while $\dot{n}_I$ results from *interference* of the two amplitudes. The expressions for $\dot{n}_{2\omega}$ and $\dot{n}_\omega$ are well known [2], and involve the imaginary parts of the even rank tensors $\chi_1(-2\omega;2\omega)$ and $\chi_3(-\omega;-\omega,\omega,\omega)$, respectively; thus they survive for any medium. On the other hand, $\dot{n}_I$ involves a third rank tensor, and therefore is nonzero only in a medium lacking center of inversion symmetry; this term was neglected in Atanasov *et al.* [6]. Using $E^i(\omega) = \bar{E}^i(\omega)\exp(i\phi^i_\omega)$ and likewise for the 2ω components, where $\bar{E}^i(\omega)$ and $\bar{E}^i(2\omega)$ are purely real, we find from (1)

$$\dot{n}_I = 2\xi_I^{ijk}(\omega)\bar{E}^i(-2\omega)\bar{E}^j(\omega)\bar{E}^k(\omega) \times \cos(\phi^j_\omega + \phi^k_\omega - \phi^i_{2\omega}),$$

where the superscripts indicate Cartesian components and

 0031-9007/99/83(20)/4192(4)$15.00

are to be summed over if repeated. Here

$$\xi_I^{ijk}(\omega) = \frac{4\pi i e^3}{(m\hbar)^3 V} \sum_{cvn\mathbf{k}} \frac{p_{vc}^i(\mathbf{k})[p_{cn}^j(\mathbf{k})p_{nv}^k(\mathbf{k}) + p_{cn}^k(\mathbf{k})p_{nv}^j(\mathbf{k})]}{\omega_{cv}^3(\mathbf{k})[\bar{\omega}_{cv}(\mathbf{k}) - \omega_n(\mathbf{k})]} \delta[\omega_{cv}(\mathbf{k}) - 2\omega]$$

is purely real; in this expression the sum over spin degeneracy is to be done as part of the sum over states. By adjusting the relative phase of the beams, $\dot{n}_I$ can be made positive or negative; of course, for a crystal initially in the ground state the total carrier injection rate $\dot{n}$ must be positive for *any* relative phase of the two beams, as is clear from (1).

This quantum interference process can be understood as a manifestation of what has come to be called coherence control [7]. In gases, coherence control of quantum state populations has been demonstrated through interference between optical transitions (e.g., single- and three-photon absorption) associated with discrete states [8–10]. For semiconductors, researchers have also tended to focus on interference control of populations through discrete states as well. Exciton populations have been coherently controlled in quantum wells [11] and quantum dots [12] using *linear* absorption via separated but phased pulses at the same frequency. Control of continuum state populations by such pulses is not possible since an induced polarization density for the inhomogeneously broadened continuum decays on the time scale of the order of the pulse width.

To gain insight into how the interference term $\dot{n}_I$ fits into the usual phenomenology of nonlinear optics and to show how energy flow is influenced, recall that in macroscopic electrodynamics the time rate of change of the energy density associated with the optical fields is $\dot{\mathbf{P}}(t) \cdot \mathbf{E}(t)$. By writing the polarization $\mathbf{P}(t) = \mathbf{P}(\omega)\exp(-i\omega t) + \text{c.c.}$, the time averaged energy density change at frequency ω is given by $\dot{\epsilon}(\omega) = -2\omega\,\mathrm{Im}[\mathbf{P}(\omega) \cdot \mathbf{E}(-\omega)]$. A similar expression holds for $\dot{\epsilon}(2\omega)$. Considering the response of the polarization to third order in the electric field and for $2\hbar\omega > E_g > \hbar\omega$, we find that each of these acquires two contributions, $\dot{\epsilon}(\omega) = -2\hbar\omega\dot{n}_\omega + \dot{\epsilon}_I(\omega)$ and $\dot{\epsilon}(2\omega) = -2\hbar\omega\dot{n}_{2\omega} + \dot{\epsilon}_I(2\omega)$. The interference terms $\dot{\epsilon}_I(\omega)$ and $\dot{\epsilon}_I(2\omega)$ are associated with $\chi_2^{ijk}(-\omega; 2\omega, -\omega)$ and $\chi_2^{ijk}(-2\omega; \omega, \omega)$, respectively, and their permutations. Since one of our fields is resonant, the overall permutation symmetry of $\chi_2^{abc}(-\omega_\beta - \omega_\gamma; \omega_\beta, \omega_\gamma)$ cannot be derived from energy conservation considerations. A careful analysis of the properties of this susceptibility tensor [13], including interband, intraband, and mixed contributions, shows that $\chi_2^{jik}(\omega; -2\omega; \omega) = [\chi_2^{ijk}(-2\omega; \omega, \omega)]^*$. Using this, along with the condition that the fields $\mathbf{P}(t)$ and $\mathbf{E}(t)$ are real, we find

$$\dot{\epsilon}_I(2\omega) - \dot{\epsilon}_I(\omega) = -8\omega\,\mathrm{Re}[\chi_2^{ijk}(-2\omega; \omega, \omega)] \times \mathrm{Im}[E^i(-2\omega)E^j(\omega)E^k(\omega)], \quad (3)$$

$$\dot{\epsilon}_I(2\omega) + \dot{\epsilon}_I(\omega) = -8\omega\,\mathrm{Im}[\chi_2^{ijk}(-2\omega; \omega, \omega)] \times \mathrm{Re}[E^i(-2\omega)E^j(\omega)E^k(\omega)]. \quad (4)$$

In a sense, Eq. (3) describes the energy transfer between fundamental and second-harmonic beams; it survives even if $\hbar\omega$ is below half the band gap, where $\mathrm{Im}[\chi_2^{ijk}(-2\omega; \omega, \omega)]$ vanishes. Equation (4) describes the positive or negative interference contribution to the absorption of light by the crystal. Using the expression for $\chi_2^{ijk}(-2\omega; \omega, \omega)$ from [13,14], and comparing with Fermi's Golden Rule calculation above, we find $\dot{\epsilon}_I(2\omega) + \dot{\epsilon}_I(\omega) = -2\hbar\omega\dot{n}_I$. Combining all of the expressions above, we find $\dot{\epsilon}(2\omega) + \dot{\epsilon}(\omega) = -2\hbar\omega\dot{n}$, as expected. The ratio $\dot{n}_I/\dot{n}$ is largest for irradiances that balance carrier generation from one- and two-photon absorption processes. Using the calculated coefficients for these processes in GaAs [6] and the calculated values for χ_2 from [14], we find that if one could take advantage of the full value of χ_2 the maximum ratio $\dot{n}_I/\dot{n}$ is 6.4% for $\hbar\omega$ corresponding to 1550 nm and increases to a value of 14% as $\hbar\omega$ approaches E_g. These values are essentially limited by how "noncentrosymmetric" the material is, as revealed by $\mathrm{Im}[\chi_2^{xyz}]$. Microscopically these modulation amplitudes are limited by the $\mathbf{k}$ dependence of the matrix elements in Eq. (2); for a given $\mathbf{k}$ vector, there is a specific ratio of irradiances and a relative phase that will give complete destructive or constructive interference. The ratio and phase are not the same for all $\mathbf{k}$ vectors, so it is not possible to simultaneously balance the arms of our matter "interferometer" for all transitions in momentum space.

The energy transfer between the two fields, as described by Eq. (3), can also play a role in carrier creation, since modification of the ω and 2ω beam irradiances can change the subsequent one- and two-photon absorption rates. For physically reasonable fundamental irradiances, this cascaded or "indirect" process is dominated by changes to the one-photon absorption rate, with a phase dependence related to $\sin(\phi_\omega^j + \phi_\omega^k - \phi_{2\omega}^i)$; the direct process varies as $\cos(\phi_\omega^j + \phi_\omega^k - \phi_{2\omega}^i)$. Note that the two processes will have a different dependence on interaction length; in the optically thin crystal limit, the direct process will vary linearly with crystal length while the indirect process will vary as the square of this length. For short interaction lengths, the carrier injection modulation is therefore expected to be primarily due to the direct interference process.

We have experimentally demonstrated the above phenomenon in GaAs at room temperature ($E_g = 1.42$ eV). The experimental setup is shown in Fig. 1. A regeneratively amplified Ti:sapphire laser operating at 250 kHz pumps an optical parametric amplifier [15] configured to produce near-bandwidth-limited 120 fs signal (1550 nm) and idler (1650 nm) pulses, each with an average power

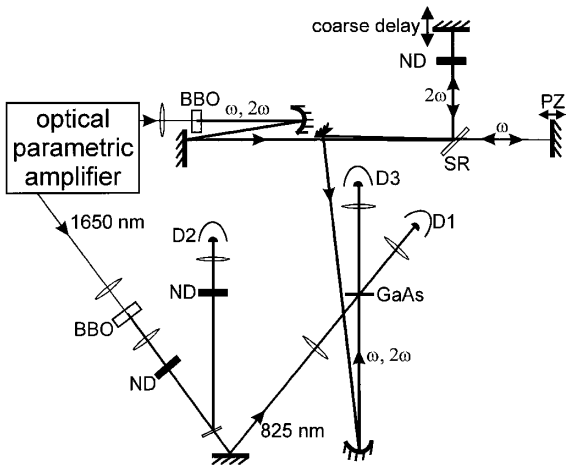

FIG. 1. Schematic diagram of experimental configuration: (ND) neutral density filter, (PZ) piezoelectric stage, (SR) short wavelength dielectric reflector, (D1,D2,D3) silicon photodetectors, and (BBO) second-harmonic generation crystal. Other filters and dielectric reflectors are not shown for purposes of clarity.

of ~8 mW. A beta barium borate (BBO) crystal is used to generate 775 nm pulses (2ω) from the signal beam (ω). Wavelengths are selected for experimental expediency and do not correspond to frequencies that would generate optimal interference modulation. The harmonically related beams are separated into distinct optical paths in an interferometer to allow the manipulation of their relative phase by a mirror (for the ω beam) driven by a piezoelectric transducer. Isolation of the two optical paths is accomplished using multiple dielectric surfaces (only one of five is shown in Fig. 1). Following the interferometer, the orthogonally polarized beams propagate collinearly before being focused onto a GaAs sample with peak incident irradiances of 9 GW cm^{-2} (1550 nm) and 150 MW cm^{-2} (775 nm). We use an undoped 650-nm-thick (111) oriented bulk GaAs sample that is van der Waals bonded to a sapphire window. For our irradiances, the rates of carrier generation by single- and two-photon absorption are nearly equivalent and the peak carrier concentration is ~10^{18} cm^{-3}. The 1550 nm beam polarization is aligned parallel to crystal $\langle 01\bar{1}\rangle$ direction to maximize the χ_2 contributions, which are determined to be $\sqrt{2/3}\,\chi_2^{xyz}$. The sample thickness is approximately equal to the energy absorption depth of the 775 nm beam, but much less than the absorption depth of the 1550 nm beam. Over the sample thickness, the phase $\phi_\omega^j + \phi_\omega^k - \phi_{2\omega}^i = 2\phi_\omega - \phi_{2\omega}$ changes by 0.6π due to linear dispersion, but this is calculated to reduce the net cross term by only 15% compared to the ideally phase-matched case.

To probe the carrier density, 825 nm pulses (second harmonic of the idler beam) are incident on the excitation spot, but delayed relative to the excitation beams by >2 ps to allow carrier cooling to be completed. The probe beam waist is 0.6 times the size of the pump beams to preferentially monitor the peak carrier density region. The probe photon energy of 1.5 eV permits one to use band-filling effects to monitor carrier density changes [16]. The 825 nm sample transmission is monitored using differential detection (D1-D2) with background-free signals obtained by the piezoelectric stage sinusoidally dithering $(2\phi_\omega - \phi_{2\omega})$ over an interval of less than π at 1 kHz and using lock-in amplification. Figure 2 (top) indicates a sinusoidal modulation of the carrier density as a function of $\omega - 2\omega$ pulse delay, as determined by the 825 nm transmission. The envelope width is determined by pulse temporal overlap. Figure 2 (bottom) shows a detail of carrier density near zero delay as a function of relative phase $(2\phi_\omega - \phi_{2\omega})$ and illustrates the expected periodicity. The density modulation amplitude is approximately 2%. Also shown is the transmission modulation of the 775 nm pump beam (as monitored by D3). The phase offset between the two curves provides a measure of the phase of the complex χ_2^{xyz}, as discussed below. To estimate the error associated with alignment and random noise sources, the experiment is repeated 10 times. The phase offset has a value of 0.35π with a standard deviation of 0.05π. The amplitude of both modulation signals as a function of 2ω beam irradiance, for fixed ω beam irradiance, gives an approximately square root dependence, consistent with the theory outlined above. Rotation of the sample around its normal yields a sixfold symmetry in the modulation amplitude as expected from the $\bar{4}3$ m symmetry of GaAs.

For an optically thin sample with no linear dispersion, carrier density modulation would be due solely to the direct process and would peak at $(2\phi_\omega - \phi_{2\omega}) = 0$. The 2ω transmission would be offset from this modulation

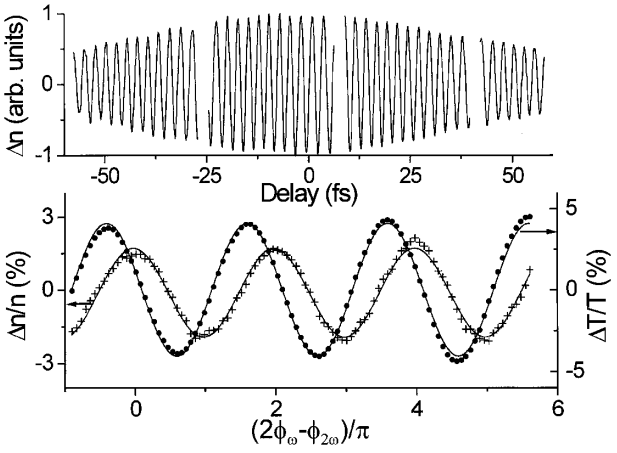

FIG. 2. (top) Phase-dependent modulated carrier density as probed by a 825 nm beam as a function of $\omega - 2\omega$ delay. Data gaps are due to limitations of experimental procedure. (bottom) Detail of modulated carrier density (crosses) and transmitted 2ω power (circles) as a function of $2\phi_\omega - \phi_{2\omega}$. Note that the zero of phase is arbitrarily chosen since it is not determined experimentally. Solid curves are best fits to the data assuming a sinusoidal shape.

trace by an amount directly related to the phase of χ_2. However, for our sample, propagation effects, including the cascaded process described above, must also be taken into account. This we have done numerically using relevant optical parameters taken from various sources [6,14,17]. The analysis uses a Green function formalism [18] to find a self-consistent solution to the electrical fields and polarization densities within the sample. Phase mismatch and Fabry-Perot effects are also included. The simulation assumes monochromatic plane waves with pulse duration much longer than the transit time of the thin film (10 fs) but shorter than the electron-hole recombination time (typically larger than 1 ns). The transmitted ω and 2ω beam irradiances, along with the generated carrier density, are determined as a function of $(2\phi_\omega - \phi_{2\omega})$. The experimentally obtained phase offset of $+1.1$ rad between the carrier density modulation and 775 nm transmission curves corresponds to a ratio of $\mathrm{Im}[\chi_2^{xyz}]/\mathrm{Re}[\chi_2^{xyz}] = 0.32 \pm 0.06$ which is in agreement with the theoretically predicted value of 0.37 [14]. Calculations also show that, for our sample thickness, the 2% modulation is dominated by the direct interference process. Phase mismatch, pump depletion, extraneous reflections, and the use of a (111) surface account for the modulation amplitude being smaller than the theoretical value (6.4%). With suitable optimization, e.g., through the use of higher frequencies or other materials including nanostructured solids, $\dot{n}_I/\dot{n}$ may be increased making unique devices or optoelectronic processes possible, including optical modulation of gain in lasers or new ultrafast switching processes.

One can distinguish control of carrier population (a scalar) from coherent control of electrical current (a vector) [19] in a semiconductor in several ways. Microscopically, current control relies on the *difference* of interference terms at $\mathbf{k}$ and $-\mathbf{k}$, while population control originates from the *sum* of the interfering transition amplitudes at $\mathbf{k}$ and $-\mathbf{k}$. The former provides a means to inject carriers into momentum space with polar distributions, corresponding to a macroscopic net flow of charge, while the latter provides a phase-dependent total carrier population. Phenomenologically, population control is related to $\chi_2(-2\omega;\omega,\omega)$ while current control arises from the most divergent part of $\chi_3(0;-2\omega,\omega,\omega)$ [20], resulting in very different dependencies on crystal symmetry, crystal cut, and beam polarizations. Current control can be observed in a medium with or without center of inversion and with near-unity efficacy of directed charge motion. However, even if present, it does not affect the transmission of the optical beams.

In conclusion, we proposed and confirmed experimentally that, when fundamental and sum-frequency beams are simultaneously present in a noncentrosymmetric medium, quantum interference effects between single- and two-photon transition amplitudes can lead to an increase or decrease of energy removal from all beams. Such an effect can be used actively to permit phase control of carrier generation and optical absorption. At a macroscopic level, these effects can be related to $\mathrm{Im}[\chi_2]$, a quantity which has largely been overlooked in the past. This process represents the lowest order effect which can be used to control continuum state populations.

The authors thank R. Atanasov, J. L. P. Hughes, A. Haché, D. Coté, and Y. Kostoulas for enlightening discussions. We acknowledge financial support from the Natural Sciences and Engineering Research Council of Canada and Photonics Research Ontario. J. M. F. acknowledges additional support from the Walter C. Sumner Foundation and H. M. vD. is grateful to the Canada Council for support.

[1] P. A. Franken, A. E. Hill, C. W. Peters, and G. Weinreich, Phys. Rev. Lett. **7**, 118 (1961).
[2] See, for example, *The Elements of Nonlinear Optics*, edited by P. N. Butcher and D. Cotter (Cambridge University Press, Cambridge, UK, 1990).
[3] N. Bloembergen, *Nonlinear Optics* (Benjamin, Reading, MA, 1965).
[4] Y. R. Shen, *The Principles of Nonlinear Optics* (Wiley, New York, 1984).
[5] R. K. Chang, J. Ducuing and N. Bloembergen, Phys. Rev. Lett. **15**, 6 (1965); H. J. Simon and N. Bloembergen, Phys. Rev. **171**, 1104 (1968).
[6] R. Atanasov, A. Haché, J. L. P. Hughes, H. M. van Driel, and J. E. Sipe, Phys. Rev. Lett. **76**, 1703 (1996).
[7] R. J. Gordon and S. A. Rice, Annu. Rev. Phys. Chem. **48**, 601 (1997).
[8] E. A. Manykin and A. M. Afanas'ev, Sov. Phys. JETP **25**, 828 (1967).
[9] D. J. Jackson and J. J. Wynne, Phys. Rev. Lett. **49**, 543 (1982).
[10] C. Chen, Y.-Y. Yin, and D. S. Elliott, Phys. Rev. Lett. **64**, 507 (1990).
[11] A. P. Heberle, J. J. Baumberg, and K. Koehler, Phys. Rev. Lett. **75**, 2598 (1995).
[12] N. H. Bonadeo, J. Erland, D. Gammon, D. Park, D. S. Katzer, and D. G. Steel, Science **282**, 1473 (1998).
[13] J. E. Sipe and A. I. Shkrebtii (unpublished).
[14] J. L. P. Hughes and J. E. Sipe, Phys. Rev. B **53**, 10 751 (1996).
[15] M. K. Reed and M. K. S. Shepard, IEEE J. Quantum Electron. **32**, 1273 (1996).
[16] Y. H. Lee, A. Chavez-Pirson, S. W. Koch, H. M. Gibbs, S. H. Park, J. Mohange, N. Peygambarian, L. Bányai, A. C. Gossard, and W. Weigmann, Phys. Rev. Lett. **57**, 2446 (1986).
[17] *Handbook of Optical Constants of Solids*, edited by E. D. Palik (Academic Press, Orlando, FL, 1985).
[18] J. E. Sipe, J. Opt. Soc. Am. B **4**, 481 (1987).
[19] A. Haché, Y. Kostoulas, R. Atanasov, J. L. P. Hughes, J. E. Sipe, and H. M. van Driel, Phys. Rev. Lett. **78**, 306 (1997); A. Haché, J. E. Sipe, and H. M. van Driel, IEEE J. Quantum Electron. **34**, 1144 (1998).
[20] C. Aversa and J. E. Sipe, IEEE J. Quantum Electron. **32**, 1570 (1996).